




# Interface disorder as the cause for the kinetic Rashba-Edelstein effect and interface spin-Hall effect at a metal-insulator boundary

A. V. Shumilin  and V. V. Kabanov   
*Jozef Stefan Institute, 1000 Ljubljana, Slovenia*

 (Received 21 June 2023; revised 21 August 2023; accepted 23 August 2023; published 26 September 2023)

The spin phenomena observed at a clean metal-insulator interface are typically reduced to the Rashba-Edelstein effect, which leads to spin accumulation over a few monolayers. We demonstrate that the presence of interface disorder significantly expands the range of potential phenomena. Specifically, the skew scattering at the metal-insulator boundary gives rise to the “kinetic Rashba-Edelstein effect,” where spin accumulation occurs on a much larger length scale comparable to the mean free path. Moreover, at higher orders of spin-orbit interaction, skew scattering is accompanied with spin relaxation resulting in the interface spin-Hall effect—a conversion of electrical current to spin current at the metal surface. Unlike the conventional spin-Hall effect, this phenomenon persists even within the Born approximation. These two predicted phenomena can dominate the spin density and spin current in devices of intermediate thickness.

DOI: [10.1103/PhysRevResearch.5.033215](https://doi.org/10.1103/PhysRevResearch.5.033215)

## I. INTRODUCTION

Spin-orbit interaction is a fundamental phenomenon that enables the exchange of angular momentum between orbital and spin degrees of freedom. One of the promising applications of this interaction is in the development of spin-orbit torque devices, which offer a scalable and field-free solution for magnetic memory that can be controlled by electrical currents [1–3]. Experimental studies have already demonstrated the magnetization switching [4–6] and domain wall motion [7] in such devices, with other potential applications including the control of magnetic skyrmions [8] and spin waves [9].

The basic setup for a spin-orbit torque device involves a magnetic bilayer composed of a heavy metal layer with strong spin-orbit coupling and a ferromagnetic layer that acts as the detector for spin polarization and spin current from the heavy metal. Although this simple bilayer composition is already functional [10], additional layers are often added to enhance or modify the device properties. These additional layers can be added from the side of the ferromagnet [11], from the side of the heavy metal [12], or between them [13]. They are usually composed of materials possessing specific spin properties, such as antiferromagnets [14] and topological insulators [15,16].

Surprisingly, recent research has shown that even insulating nonmagnetic molecules can significantly enhance the spin torque when added from the side of the heavy metal, for heavy metal thicknesses up to 5 nm [17]. These results have drawn our attention to the spin phenomena occurring at the interface between heavy metals and insulators.

Spin generation in magnetic bilayers is typically attributed to either the Rashba-Edelstein surface effect or the spin-Hall effect (see Fig. 1). Although it can be difficult to distinguish between these effects in a given experiment [4], they differ significantly in terms of the device engineering. The Rashba-Edelstein effect results in spin polarization at the surface of the heavy metal where inversion symmetry is broken. However, this polarization is confined to only a few monolayers near the interface [18–21], meaning that the spin generated at the heavy metal interface with a third material can affect the ferromagnetic layer only in very thin devices. When the heavy metal layer is thick, the spin torque in the ferromagnetic layer is usually attributed to the spin-Hall effect, which is the conversion of electrical current to spin current in the heavy metal layer [22,23]. However, the spin-Hall effect is related to the bulk properties of the heavy metal [24–26] and is not expected to be significantly influenced by the heavy-metal-insulator interface. In relatively clean samples the spin-Hall effect is dominated by skew scattering at impurities in the bulk, which is absent in the Born approximation, resulting in a suppression factor of  $V_0/\varepsilon_F$ , where  $V_0$  is the potential of a single impurity and  $\varepsilon_F$  is the Fermi energy.

The recently predicted interface spin-Hall effect combines the properties of the Rashba-Edelstein and conventional spin-Hall effects. It refers to the electrical-current-to-spin-current conversion at the interface. Its phenomenological possibility is demonstrated in Refs. [27–29]. However, it has only been studied for the interface of two metals and was attributed to spin filtering, which involves different probabilities for spin-up and spin-down electrons to traverse the interface between metals [2,30,31]. Similar spin filtering was also predicted for tunneling through semiconductor barriers [32–34].

Here we investigate the spin kinetics near a disordered heavy-metal-insulator interface. We demonstrate that the disorder significantly increases the variety of interface spin phenomena. Skew scattering at the interface impurities causes

*Published by the American Physical Society under the terms of the Creative Commons Attribution 4.0 International license. Further distribution of this work must maintain attribution to the author(s) and the published article's title, journal citation, and DOI.*

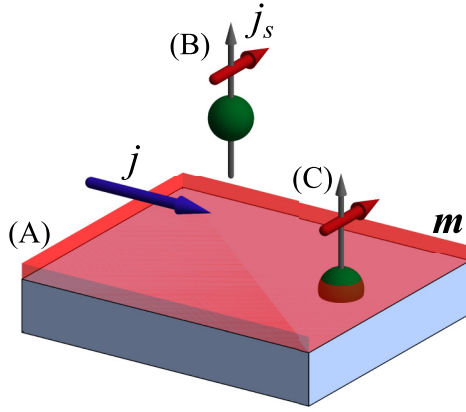


FIG. 1. The three phenomenological effects leading to the spin polarization in the heavy metal layer. Letter (A) denotes the Rashba-Edelstein effect; letter (B) means the spin-Hall effect; and (C) denotes the interface spin-Hall effect. The blue arrow stands for the direction of the electrical current. Gray arrows show the direction of spin flow. The red arrows correspond to the direction of spin polarization. Green spheres depict the impurities.

spin accumulation over a distance comparable to the mean free path from the interface. This phenomenologically corresponds to the Rashba-Edelstein effect; however, the thickness of the spin accumulation layer is significantly larger than that predicted in Refs. [19,20]. Combined with spin relaxation, this leads to the interface spin-Hall effect, which is absent at a clean metal-insulator interface. Both of these phenomena are sensitive to the materials that make up the interface and their properties, as well as their disorder.

## II. MODEL OF THE HEAVY METAL SURFACE

We consider a clean heavy metal interface with an insulator described by the model Hamiltonian

$$\hat{H} = \frac{\hat{\mathbf{p}}^2}{2m} + U(z) - \gamma \frac{\partial U}{\partial z} (\sigma_x \hat{p}_y - \sigma_y \hat{p}_x). \quad (1)$$

Here,  $\hat{\mathbf{p}} = -i\hbar\nabla$  is the momentum operator,  $m$  is the effective mass, and  $U(z) = U_0\theta(z)$  is the potential energy describing the abrupt barrier at  $z = 0$  with the height  $U_0$ .  $\gamma$  is the effective spin-orbit interaction inside the heavy metal. Its solution in Appendix A leads to the following electron wave function on the metal side of the interface:

$$\Psi_\alpha(\mathbf{k}) = \frac{e^{i\mathbf{k}_\perp \mathbf{r}_\perp}}{\sqrt{2V}} (e^{i|k_z|z} + \hat{r}(\mathbf{k})e^{-i|k_z|z})u_\alpha. \quad (2)$$

Here,  $\mathbf{k}$  is the electron wave vector,  $k_z$  is its component along  $z$ ,  $\mathbf{k}_\perp$  is its  $xy$  component, and  $u_\alpha$  is an arbitrary spinor. Equation (2) includes the spin-dependent reflection amplitude  $\hat{r}(\mathbf{k})$ :

$$\hat{r}(\mathbf{k}) = -e^{2i\phi_0} [\cos(\Delta\phi)\hat{1} + i\sin(\Delta\phi)\hat{\sigma}_k], \quad (3)$$

where  $\phi_0 = (\phi_+ + \phi_-)/2$  is the average phase change during the reflection and  $\Delta\phi = \phi_+ - \phi_-$  shows its spin dependence.  $\phi_\pm = \arctan[k_z/(\kappa \mp 2m\gamma U_0 k_\perp/\hbar)]$ , and  $\kappa = \sqrt{2mU_0/\hbar^2 - k_z^2}$ .

$\hat{\sigma}_k$  is the combination of Pauli matrices:

$$\hat{\sigma}_k = \frac{k_y}{|k_\perp|}\hat{\sigma}_x - \frac{k_x}{|k_\perp|}\hat{\sigma}_y. \quad (4)$$

It is demonstrated in Appendix A that in agreement with previous studies [19,20] the clean interface does not exhibit an interface spin-Hall effect and the spin polarization is confined to several monolayers.

The primary objective of this study is to incorporate interface disorder into the theory. The most common approach to the electron kinetics near a disordered interface involves finite probabilities of specular and nonspecular reflection [35]. However, to address the new spin phenomena it is crucial to consider a microscopic mechanism responsible for nonspecular reflection. Two conventional approaches exist for modeling reflection from disordered interfaces: roughness of the interface [36,37] and interface impurities [38–40]. Both approaches allow for the possibility of nonspecular reflection, and we consider them to be interchangeable. In this paper we adopt the latter one.

A single impurity can be described with potential energy  $V_0(\mathbf{r})$ . With respect to the spin-orbit interaction it leads to the additional term in the electron Hamiltonian

$$V(\mathbf{r}) = V_0(\mathbf{r}) + \gamma\sigma \left[ \frac{\partial V_0}{\partial \mathbf{r}} \times \mathbf{p} \right]. \quad (5)$$

In this paper we consider small impurities with  $V_0(\mathbf{r}) = V_I\delta(\mathbf{r})$ , where  $V_I$  stands for the magnitude of the impurity potential.

The scattering from the impurities is characterized by the matrix elements  $\hat{V}(\mathbf{k}_1, \mathbf{k}_2) = V_{\alpha\beta}(\mathbf{k}_1, \mathbf{k}_2) = \langle \Psi_\alpha(\mathbf{k}_1) | V(\mathbf{r}) | \Psi_\beta(\mathbf{k}_2) \rangle$ , where  $\Psi_\alpha(\mathbf{k}_1)$  and  $\Psi_\beta(\mathbf{k}_2)$  correspond to the electron states at the clean interface, as described by Eq. (2). In order to analyze the scattering process, it is useful to decompose the scattering elements into two terms:

$$\hat{V}(\mathbf{k}_1, \mathbf{k}_2) = \hat{V}^{(N)}(\mathbf{k}_1, \mathbf{k}_2) + \hat{V}^{(SO)}(\mathbf{k}_1, \mathbf{k}_2), \quad (6a)$$

$$V_{\alpha\beta}^{(N)}(\mathbf{k}_1, \mathbf{k}_2) = \frac{1}{2} \frac{V_I}{V} (1 + \hat{r}^+(\mathbf{k}_1))(1 + \hat{r}(\mathbf{k}_2)), \quad (6b)$$

$$\begin{aligned} \hat{V}^{(SO)}(\mathbf{k}_1, \mathbf{k}_2) = & \frac{iV_I\gamma}{2\hbar V} (\sigma[\mathbf{p}_1^{(\text{inc})} \times \mathbf{p}_2^{(\text{inc})}] \\ & + \hat{r}^+(\mathbf{k}_1)\sigma[\mathbf{p}_1^{(\text{ref})} \times \mathbf{p}_2^{(\text{inc})}] \\ & + \sigma[\mathbf{p}_1^{(\text{inc})} \times \mathbf{p}_2^{(\text{ref})}]\hat{r}(\mathbf{k}_2) \\ & + \hat{r}^+(\mathbf{k}_1)\sigma[\mathbf{p}_1^{(\text{ref})} \times \mathbf{p}_2^{(\text{ref})}]\hat{r}(\mathbf{k}_2)). \end{aligned} \quad (6c)$$

Here,  $V_{\alpha\beta}^{(N)}(\mathbf{k}_1, \mathbf{k}_2)$  corresponds to the first term on the right-hand side of Eq. (5), and  $V_{\alpha\beta}^{(SO)}(\mathbf{k}_1, \mathbf{k}_2)$  is related to the spin-orbit correction and to the second term on the right-hand side of Eq. (5).  $\mathbf{p}^{(\text{inc})} = \hbar(k_x, k_y, |k_z|)$  is the momentum of the incident electron, and  $\mathbf{p}^{(\text{ref})} = \hbar(k_x, k_y, -|k_z|)$  is the momentum of the reflected electron.  $\hat{r}^+(\mathbf{k})$  is the Hermitian conjugate of the reflection amplitude described with Eq. (3).

Equations (6b) and (6c) can be represented as the four different reflection possibilities shown in Fig. 2(a). The electron can undergo scattering from the impurity without interaction with the surface, or can be specularly reflected before or after the scattering or both.

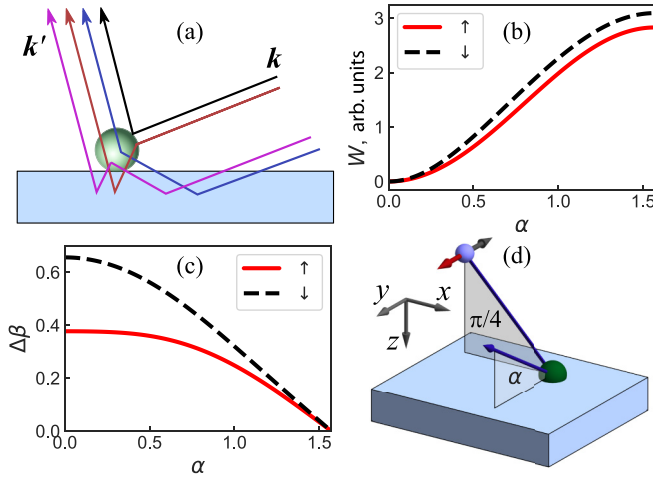


FIG. 2. (a) The four possibilities for the impurity scattering from state  $\mathbf{k}$  to the state  $\mathbf{k}'$  in the presence of the interface. (b) The spin dependence of the scattering amplitude. (c) Asymmetric spin rotation angle. The results presented in (b) and (c) correspond to  $U_0/\varepsilon_F = 4$ ,  $\gamma p_F^2/\hbar = 0.2$  and to the geometry shown in (d).

The probability of scattering depends on the quantum interference between the different reflection possibilities, which can be constructive or destructive depending on the phase  $\varphi_0 \pm \Delta\varphi$  and the relation between  $\hat{V}^{(N)}$  and  $\hat{V}^{(SO)}$ . This probability varies for different spin projections, leading to skew scattering and spin separation at the surface. Figure 2(b) shows the probability for electrons with an incident angle of  $\pi/4$  in the  $xz$  plane to scatter to the  $yz$  plane. The scattering rate depends on the spin projection to the  $y$  axis. The calculation details are presented in Appendix B. When spin-orbit interaction is present, electron scattering also results in spin rotation, leading to spin relaxation after multiple random scattering events [37]. Figure 2(c) demonstrates that in our case, this rotation becomes asymmetric, causing a spin-up electron to rotate differently from a spin-down electron. This asymmetric spin rotation produces spin polarization of reflected electrons, even when the incident electrons are not spin polarized, resulting in the interface spin-Hall effect. The geometry corresponding to Figs. 2(b) and 2(c) is shown in Fig. 2(d).

### III. SPIN CURRENT AND SPIN POLARIZATION

To understand the impact of the skew scattering and asymmetric spin rotation on the electrons in the bulk of the heavy metal, we introduce the Boltzmann equation

$$\frac{\partial \hat{f}(\mathbf{r}, \mathbf{p})}{\partial t} + \mathbf{v} \frac{\partial \hat{f}(\mathbf{r}, \mathbf{p})}{\partial \mathbf{r}} + \mathbf{F} \frac{\partial \hat{f}(\mathbf{r}, \mathbf{p})}{\partial \mathbf{p}} = I(\hat{f}(\mathbf{r}, \mathbf{p})). \quad (7)$$

Here, the distribution function  $\hat{f}(\mathbf{r}, \mathbf{p})$  is a  $2 \times 2$  matrix in spin space that depends on the coordinate and momentum as usual.  $I(\hat{f}(\mathbf{r}, \mathbf{p}))$  is the scattering operator.

We consider the following ansatz for the distribution function:  $\hat{f} = \hat{f}_0 + \hat{f}_1 + \hat{f}_2$ . Here,  $\hat{f}_0$  is the equilibrium electron distribution. It is proportional to the unit matrix  $\hat{1}$  in the spin

space.

$$\hat{f}_1 = -\frac{j}{e} \frac{p_x}{n} \frac{\partial \hat{f}_0}{\partial \varepsilon} \quad (8)$$

represents the electric current density  $j$ , which is assumed to flow along the  $x$  axis.  $\hat{f}_2$  describes the spin polarization. We assume  $\hat{f}_2 \ll \hat{f}_1 \ll \hat{f}_0$ , which corresponds to a relatively small spin polarization due to the skew scattering. In this case it is possible to neglect  $\hat{f}_2$  for the incident electrons, because it would lead only to a small correction for  $\hat{f}_2$  of scattered electrons (that is responsible for the kinetic Rashba-Edelstein and interface spin-Hall effects).

The skew scattering should be introduced into Boltzmann equation as a boundary condition. It is derived in Appendix C and reads

$$\hat{f}_2(\mathbf{p}, z=0) = \frac{mV}{S|p_z|} \hat{r}(\mathbf{p}) \left( \int \frac{V d\mathbf{p}'}{(2\pi\hbar)^3} \times \widehat{\mathcal{W}}\left(\frac{\mathbf{p}}{\hbar}, \frac{\mathbf{p}'}{\hbar}\right) (f_1(\mathbf{p}') - f_1(\mathbf{p})) \right) \hat{r}(\mathbf{p})^+. \quad (9)$$

Here,

$$\widehat{\mathcal{W}}(\mathbf{k}, \mathbf{k}') = \frac{2\pi}{\hbar} N_I \widehat{V}(\mathbf{k}, \mathbf{k}') \widehat{V}(\mathbf{k}', \mathbf{k}) \delta(\varepsilon_k - \varepsilon_{k'}), \quad (10)$$

where  $N_I$  is the total number of impurities.

Equations (C3) and (C4) show that  $f_2$  is proportional to the two-dimensional impurity concentration  $N_I/S$  which controls the probability  $P_{\text{nsp}}$  that an incident electron with Fermi energy is reflected nonspecularly. This probability, averaged over incident electron momenta, can be expressed as follows:

$$P_{\text{nsp}} = \frac{4\pi^2 \hbar^3}{S p_F^2} \mathcal{I}_N, \quad (11a)$$

$$\mathcal{I}_N = \iint \frac{V^2 d\mathbf{p} d\mathbf{p}'}{(2\pi\hbar)^6} \text{Tr} \widehat{\mathcal{W}}\left(\frac{\mathbf{p}}{\hbar}, \frac{\mathbf{p}'}{\hbar}\right) \delta(\varepsilon - \varepsilon_F). \quad (11b)$$

In our model the macroscopic symmetry in the  $xy$  plane is not broken, and the only possible spin current density  $j_s$  in the  $z$  direction describes the flow of  $y$ -polarized spins. It is conventionally expressed with the interface spin-Hall angle

$$\tan \theta_{\text{sH}} = \frac{j_s}{j/e} = \frac{3}{4} P_{\text{nsp}} \frac{\mathcal{I}_{\text{sH}}}{\mathcal{I}_N}, \quad (12a)$$

$$\mathcal{I}_{\text{sH}} = \int \frac{V^2 d\mathbf{p} d\mathbf{p}'}{(2\pi\hbar)^6} \left( \frac{p'_x}{p_F} - \frac{p_x}{p_F} \right) \delta(\varepsilon - \varepsilon_F) \times \text{Tr} \hat{\sigma}_y \left[ \hat{r}(\mathbf{p}) \widehat{\mathcal{W}}\left(\frac{\mathbf{p}}{\hbar}, \frac{\mathbf{p}'}{\hbar}\right) \hat{r}^+(\mathbf{p}) \right]. \quad (12b)$$

The interface spin-Hall angle calculated with Eq. (12) is shown in Fig. 3(a) as a function of spin-orbit interaction for different barrier heights  $U_0$ . Interestingly,  $\theta_{\text{sH}}$  is not an odd function of  $\gamma$ . It is related to the electron momentum  $\mathbf{p}$  being an operator that does not commute with impurity potential  $V_0(\mathbf{r})$ . Figure 3(b) shows the  $\theta_{\text{sH}}(\gamma)$  dependence in the double logarithm scale for  $U_0 = 10\varepsilon_F$  and small positive  $\gamma$ . The spin-Hall angle is a high-order function of  $\gamma$ :  $\theta_{\text{sH}} \propto \gamma^3$  at very small  $\gamma$  and becomes steeper with an increase in  $\gamma$ , up to  $\theta_{\text{sH}} \propto \gamma^6$ . As shown in Fig. 3(a) there is a maximum in this dependence corresponding to  $\gamma p_F^2/\hbar \sim \sqrt{\varepsilon_F/U_0}$ .

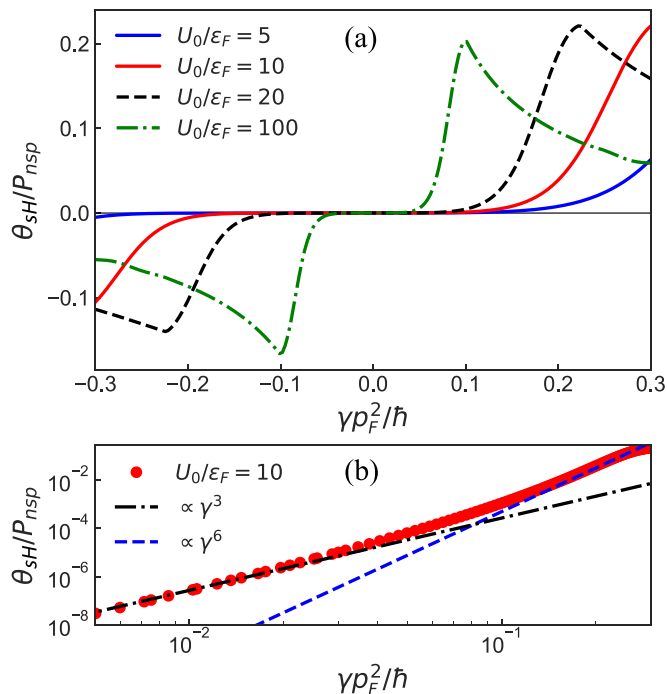


FIG. 3. (a) Interface spin-Hall angle as a function of spin-orbit interaction for various relationships between interface potential and Fermi energy  $U_0/\varepsilon_F$  as shown in the legend. (b) The  $\theta_{\text{SH}}(\gamma)$  dependence for  $U_0/\varepsilon_F = 10$  in the double logarithm scale. The blue dashed line and the black dash-dotted line correspond to  $\theta_{\text{SH}} \propto \gamma^6$  and  $\theta_{\text{SH}} \propto \gamma^3$ , respectively.

The physical mechanism of the interface spin-Hall effect consists of two parts. The first one is the skew scattering shown in Fig. 2(b). However, the skew scattering alone is insufficient to generate the spin current if spin is conserved during the scattering. Therefore the interface spin-Hall effect requires also the asymmetric spin rotation shown in Fig. 2(c) that leads to the “spin relaxation” which depends on spin projection. The spin relaxation is a second order in  $\gamma$  phenomenon [37], meaning that the interface spin-Hall effect is absent in the first-order approximation over  $\gamma$ .

To show that the spin separation itself is a first-order effect, we examine the spin accumulation near the interface. We solve the Boltzmann equation using the minimal model, which assumes that the scattering operator in the bulk can be described by a single relaxation time  $\tau$ :  $I(\hat{f}) = (\hat{f}_0 - \hat{f})/\tau$ . By applying this assumption to Eq. (7), we obtain the solution

$$\hat{f}_2(\mathbf{p}, z) = \hat{f}_2(\mathbf{p}, 0) \exp\left(-\frac{z p_F}{p_z l_{\text{free}}}\right). \quad (13)$$

Here,  $l_{\text{free}} = v_F \tau$  is the mean free path.

The spin polarization calculated from Eq. (13) reads

$$m_y(z) = \frac{3}{4} \frac{j}{e v_F} P_{\text{nsp}} \frac{\mathcal{I}_s(z)}{\mathcal{I}_N}, \quad (14a)$$

$$\begin{aligned} \mathcal{I}_s(z) = & \int \frac{V^2 d\mathbf{p} d\mathbf{p}'}{(2\pi\hbar)^6} \text{Tr}_{\sigma_y} \hat{r}(\mathbf{p}) \hat{\mathcal{W}}\left(\frac{\mathbf{p}}{\hbar}, \frac{\mathbf{p}'}{\hbar}\right) \hat{r}^+(\mathbf{p}) \\ & \times \left(\frac{p'_x}{|p_z|} - \frac{p_x}{|p_z|}\right) \exp\left(-\frac{z p_F}{l_{\text{free}} |p_z|}\right) \delta(\varepsilon - \varepsilon_F). \end{aligned} \quad (14b)$$

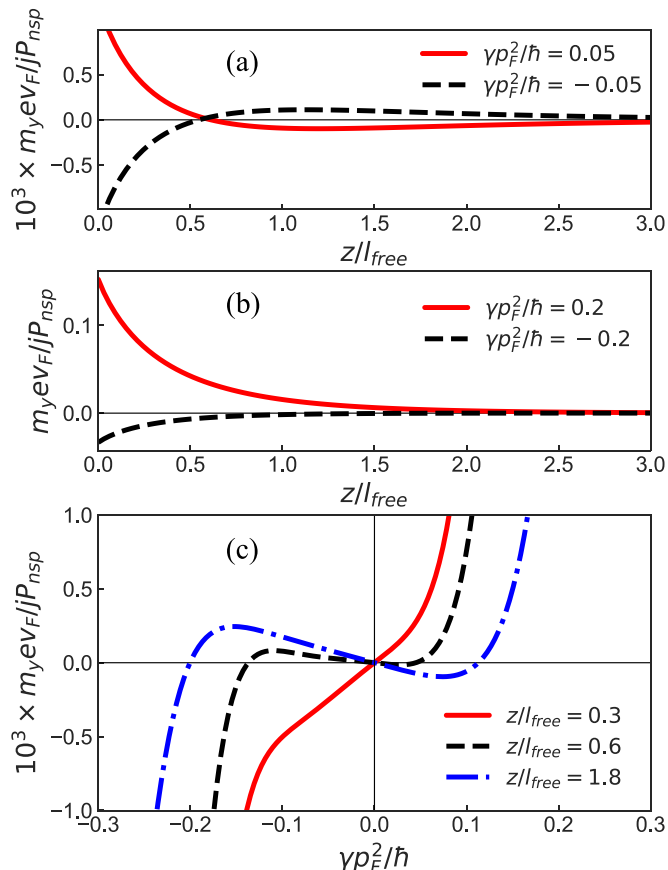


FIG. 4. Spin accumulation  $m_y$  due to the kinetic Rashba-Edelstein effect calculated for  $U_0 = 10\varepsilon_F$ . (a) and (b) show the dependence  $m_y(z)$  for different values of  $\gamma$ . (c) shows the dependence of accumulated spin on the spin-orbit interaction parameter  $\gamma$  for three different values  $z/l_{\text{free}}$ .

Figure 4 shows the spin polarization  $m_y$  calculated for  $U_0 = 10\varepsilon_F$ . Similarly to the interface spin-Hall effect, the polarization obtained from the Boltzmann equation appears only due to the possibility of nonspecular reflection and is normalized by  $P_{\text{nsp}}$ . Figures 4(a) and 4(b) show the  $m_y$  distribution over  $z$  for  $\gamma p_F^2/\hbar = \pm 0.05$  and  $\gamma p_F^2/\hbar = \pm 0.2$ , respectively. For small values of  $\gamma$ ,  $m_y$  changes its sign as a function of  $z$  indicating the difference in the average reflection angle for different spin projections. This change of the sign disappears at larger values of  $\gamma$  when the interface spin-Hall effect becomes sufficiently strong to dominate the spin accumulation.

Phenomenologically, the calculated spin accumulation is the Rashba-Edelstein effect because it is confined near the interface. However, unlike the conventional Rashba-Edelstein effect at clean interfaces studied in Refs. [19,20], the polarization spans up to the mean free path  $l_{\text{free}}$ . In the case where the sample only contains impurities at the surface and the bulk is clean,  $l_{\text{free}}$  can be arbitrary large. Thus the resulting spin polarization can be referred to as the kinetic Rashba-Edelstein effect.

#### IV. DISCUSSION

The interface spin-Hall and kinetic Rashba-Edelstein effects are closely related to the interference of different

reflected waves shown in Fig. 2(a). Both effects should disappear if this interference is somehow suppressed. For example, one can consider bulk impurities near the interface as a possible reason for the interface spin-Hall effect. However, in this case the phase of the reflection amplitude  $\hat{r}$  would be modified by the random distance between the impurity and the surface. If this distance exceeds  $\hbar/p_F$ , the interference and the spin generation would be suppressed. Nevertheless, if the impurities are located precisely at the interface and are small compared with  $p_F$ , their potential  $V_I$  is not significant: It is absorbed into nonspecular reflection probability  $P_{\text{nsr}}$  in our final expressions. This is a consequence of the calculations being performed within the Born approximation. We presume that introduction of complex impurities with large size and high potential energy can significantly modify the spin accumulation and spin current.

The existence of the interface spin-Hall effect in the Born approximation makes it fundamentally different from the ordinary spin-Hall effect that appears only as a higher-order correction over the impurity potential  $V_I$  and is suppressed if the disorder is Gaussian. Although there are some predicted mechanisms for its existence in Gaussian disorder, namely the combined scattering from impurities and phonons [41] and the scattering at close impurity complexes [41,42], all these mechanisms require high orders of perturbation theory. The interface spin-Hall effect is possible in the Born approximation because of the large interface potential energy that exists already in zeroth order.

The unusual properties of the kinetic Rashba-Edelstein effect and interface spin-Hall effect suggest that in some cases the predicted interface phenomena should dominate the spin accumulation and spin current. It happens when the thickness  $d$  of the sample is intermediate, i.e.,  $\hbar/p_F \ll d \lesssim l_{\text{free}}$ , and bulk impurities that control conductivity have small potential energy  $V_0 \ll \epsilon_F$ . If these conditions are met, the control of interface properties is important to optimize the spin torque. The effect of interface roughness is sometimes reported in experiments [17,43]; however, to the best of our knowledge, there have been no systematic studies. We predict that the perfect interface is not necessarily a clean one. Controlled

disorder can serve as a source of both spin polarization and spin current. It allows one to control the functionality of spin torque devices by surface engineering, i.e., by manipulating surface impurity concentration and their type. Furthermore, the sensitivity of the interface spin-Hall effect to the interface potential  $U_0$  provides a means of controlling spin torque with gating.

In conclusion, our study demonstrates that impurities at the metal-insulator interface significantly increase the variety of surface spin effects. The skew scattering from these impurities induces spin accumulation that extends up to the mean free path. When combined with spin relaxation, it gives rise to the interface spin-Hall effect, which converts charge currents to spin currents at the metal-insulator boundary.

### ACKNOWLEDGMENTS

We have received funding from the European Community's H2020 program under Grant Agreement INTERFAST (H2020-FET-OPEN-965046) and from Slovenian Research Agency Program No. P1-0040.

### APPENDIX A: SPIN POLARIZATION NEAR THE CLEAN INTERFACE

Our starting point is the Hamiltonian described by Eq. (1). We are interested in its solutions when the electron energy  $\epsilon$  is below the barrier  $U_0$ . We start with rotation in the spin space with the matrix

$$U_\sigma = \begin{pmatrix} \tilde{k}_\perp & -\tilde{k}_\perp \\ 1 & 1 \end{pmatrix}, \quad (\text{A1})$$

where  $\tilde{k}_\perp = (ik_x + k_y)/k_\perp$ ,  $k_\perp = \sqrt{k_x^2 + k_y^2}$ . After the canonical transformation  $U_\sigma^{-1} H U_\sigma$  the Hamiltonian becomes diagonal:

$$H = -\frac{\hbar^2}{2m} \frac{d^2}{dz^2} + \frac{\hbar^2 k_\perp^2}{2m} + U_0 \theta(z) \mp \gamma U_0 \delta(z) k_\perp. \quad (\text{A2})$$

Using Eq. (A2), we find the eigenfunctions

$$\psi_\pm(\mathbf{r}_\perp, z) = \begin{cases} A_\pm \begin{pmatrix} \pm \tilde{k}_\perp \\ 1 \end{pmatrix} \sin(k_\pm z - \phi_\pm) \exp(i\mathbf{k}_\perp \mathbf{r}_\perp), & z < 0 \\ -A_\pm \begin{pmatrix} \pm \tilde{k}_\perp \\ 1 \end{pmatrix} \sin(\phi_\pm) \exp(i\mathbf{k}_\perp \mathbf{r}_\perp) \exp(-\kappa z), & z > 0. \end{cases} \quad (\text{A3})$$

Here,  $A_\pm = \sqrt{\frac{\kappa_\pm}{\kappa_\pm L + 1}}$ ,  $\kappa = \sqrt{\frac{2m(U_0 - \epsilon_\pm)}{\hbar^2}}$ ,  $\kappa_\pm = \kappa \mp \frac{2m\gamma U_0 k_\perp}{\hbar^2}$ ,  $\epsilon_\pm = \frac{\hbar^2 k_\pm^2}{2m}$ , and  $L$  is the size of the sample in the  $z$  direction that corresponds to the thickness of the heavy metal layer.  $k_\pm$  is the electron wave vector in the  $z$  direction, which becomes spin dependent after the effects of finite  $L$  are taken into account. The phase shift  $\phi_\pm$  is determined by the equation  $\tan \phi_\pm = k_\pm / \kappa_\pm$ . The energy is

$$\epsilon_\pm = \frac{\hbar^2 k_\pm^2}{2m} + \frac{\hbar^2 k_\perp^2}{2m}. \quad (\text{A4})$$

To describe the boundary conditions for the Boltzmann equation, it is enough to consider the infinite sample  $L \rightarrow \infty$ . In this case,  $k_+ = k_- = k_z$ ,  $\epsilon_+ = \epsilon_- = \epsilon_k$ , and the solution of the Schrödinger equation exists for an arbitrary incident wave.

$$\begin{pmatrix} a \\ b \end{pmatrix} \exp(ik_z z) \exp(i\mathbf{k}_\perp \mathbf{r}_\perp). \quad (\text{A5})$$

Here,  $(a, b)$  is an arbitrary spinor. According to Eq. (A3), its reflected wave is described as follows:

$$\hat{r}(k) \begin{pmatrix} a \\ b \end{pmatrix} \exp(-ik_z z) \exp(i\mathbf{k}_\perp \mathbf{r}_\perp). \quad (\text{A6})$$

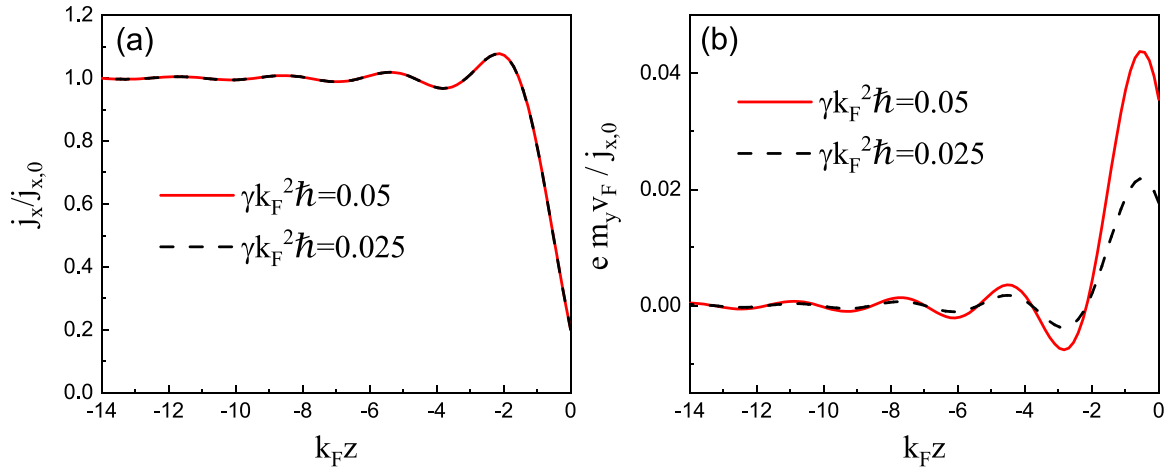


FIG. 5. The distribution of the current density near the surface (a) and spin density as a function of  $z$  (b).

Here,

$$\hat{r}(k) = \exp(i\pi + 2i\phi_0)(\cos(\Delta\phi)\hat{\sigma}_0 + i\sin(\Delta\phi)\hat{\sigma}_k), \quad (\text{A7})$$

$$\hat{\sigma}_k = \frac{k_y}{|k_\perp}\hat{\sigma}_x - \frac{k_x}{|k_\perp}\hat{\sigma}_y. \quad (\text{A8})$$

Interestingly, to account for the Rashba-Edelstein effect at the clean interface, it is important to consider  $L$  to be finite. Here, we assume the boundary conditions at  $z = -L$ :  $d\psi(\mathbf{r}_\perp, z)/dz|_{z=-L} = 0$ . This leads to the following equations for  $k_\pm$  and  $\phi_\pm$ :

$$k_\pm = \frac{\pi}{2L}(2n+1) - \frac{\phi_\pm}{L},$$

$$\phi_\pm = \arctan\left[\frac{(n+1/2)\pi - \phi_\pm}{Lk_\pm}\right], \quad (\text{A9})$$

where  $n$  is an arbitrary integer. Equations (A4) and (A9) show that when  $L$  is finite, the discrete levels for spin up and spin down are different, which will later lead to the current-induced spin polarization.

To account for the in-plane electric current, we introduce the distribution function of the electrons  $f(\mathbf{k}) = f_0(\varepsilon - v\hbar k_x)$ . Here,  $f_0$  is the Fermi function, and  $v$  is the drift velocity that is assumed to be along the  $x$  direction. The current density  $j_x(z)$  is defined as follows:

$$j_x(z) = \frac{e}{L} \sum_n \int \frac{d\mathbf{k}_\perp}{(2\pi)^2} \frac{2\hbar k_x}{m} [\sin(k_+z - \phi_+)^2 f_0(\varepsilon_+ - \hbar v k_x) + \sin(k_-z - \phi_-)^2 f_0(\varepsilon_- - \hbar v k_x)]. \quad (\text{A10})$$

Note that although the distribution  $f(\mathbf{k})$  does not depend on spin, the energies  $\varepsilon_\pm$  do.

Equation (A10) can be simplified by expanding the Fermi functions over small  $v k_x$  and integrating over the angle of  $\mathbf{k}_\perp$ .

$$j_x(z) = \frac{ev\hbar^2}{8\pi mTL} \sum_n \int dk_\perp k_\perp^3 \times \left[ \frac{\sin^2(k_+z - \phi_+)}{\cosh^2\left(\frac{\varepsilon_+ - \mu}{2T}\right)} + \frac{\sin^2(k_-z - \phi_-)}{\cosh^2\left(\frac{\varepsilon_- - \mu}{2T}\right)} \right]. \quad (\text{A11})$$

Here,  $T$  is the temperature and  $\mu$  is the chemical potential. Equation (A11) describes the distribution of the current density near the interface.

To describe the spin polarization, we take into account that

$$(\pm\tilde{k}_\perp^*, 1)\sigma_y \begin{pmatrix} \pm\tilde{k}_\perp \\ 1 \end{pmatrix} = \mp 2k_x/k_\perp. \quad (\text{A12})$$

This allows us to derive the expression for the distribution of spin polarization  $m_y(z)$ :

$$m_y(z) = \frac{1}{L} \sum_n \int \frac{d\mathbf{k}_\perp}{(2\pi)^2} \frac{2k_x}{k_\perp} [\sin(k_+z - \phi_+)^2 f_0(\varepsilon_+ - \hbar v k_x) - \sin(k_-z - \phi_-)^2 f_0(\varepsilon_- - \hbar v k_x)]. \quad (\text{A13})$$

After expanding this equation over small  $v k_x$  and performing the angle integration, we obtain

$$m_y(z) = \frac{v\hbar}{8\pi TL} \sum_n \int dk_\perp k_\perp^2 \times \left[ \frac{\sin^2(k_+z - \phi_+)}{\cosh^2\left(\frac{\varepsilon_+ - \mu}{2T}\right)} - \frac{\sin^2(k_-z - \phi_-)}{\cosh^2\left(\frac{\varepsilon_- - \mu}{2T}\right)} \right]. \quad (\text{A14})$$

This formula describes the spin accumulation near the interface when current is flowing parallel to the surface. Figure 5 represents the calculated current density and the accumulated spin density as a function of  $z$  (Rashba-Edelstein effect). The current density is normalized to  $j_{x,0} = evk_F^3/3\pi^2$ , which is the current density far from the interface. Figure 5 shows that in a clean sample the spin polarization exists only at the distances  $\sim \hbar/p_F$  from the surface where the current is modified by quantum effects.

Note also that the wave functions (A3) do not include density flux  $\text{Im}\psi_\pm^* \nabla \psi_\pm = 0$  and the spin density (A14) is not accompanied by spin current.

## APPENDIX B: SPIN-DEPENDENT SCATTERING AT THE INTERFACE IMPURITIES

In the general case, impurity scattering requires the density matrix formalism for its description. The usual procedure for such a description starts with the density matrix  $\hat{\rho}(\mathbf{k})$  diagonal in the space of wave functions  $\Psi_{\mathbf{k}}$  and considers nondiagonal

terms  $\hat{\rho}(\mathbf{k}, \mathbf{k}')$  as a small perturbation. However, the terms  $\hat{\rho}(\mathbf{k})$  diagonal in the space of  $\Psi_{\mathbf{k}}$  are still  $2 \times 2$  matrices in spin space. The master equation for the density matrix reads

$$\frac{\partial \hat{\rho}}{\partial t} = \frac{i}{\hbar} (\hat{\rho} \hat{V} - \hat{V} \hat{\rho}). \quad (\text{B1})$$

Here,  $\hat{V}$  is the impurity energy that includes both potential energy and spin-orbital correction (6).

We assume the slow variance of diagonal matrix elements compared with the oscillation frequencies  $(\varepsilon_{\mathbf{k}} - \varepsilon_{\mathbf{k}'})/\hbar$ . This allows us to derive an expression for the perturbation  $\hat{\rho}(\mathbf{k}, \mathbf{k}')$  from Eq. (B1):

$$\hat{\rho}(\mathbf{k}, \mathbf{k}') = \frac{\exp(i \frac{\varepsilon_{\mathbf{k}} - \varepsilon_{\mathbf{k}'}}{\hbar} t)}{\varepsilon_{\mathbf{k}} - \varepsilon_{\mathbf{k}'} - i\delta} \times (\hat{\rho}(\mathbf{k}) \hat{V}(\mathbf{k}\mathbf{k}') - \hat{V}(\mathbf{k}\mathbf{k}') \hat{\rho}(\mathbf{k}')). \quad (\text{B2})$$

This equation should be substituted back into Eq. (B1), where we now keep only the nonoscillating terms:

$$\begin{aligned} \frac{\partial \hat{\rho}(\mathbf{k})}{\partial t} &= \sum_{\mathbf{k}'} \frac{i/\hbar}{\varepsilon_{\mathbf{k}'} - \varepsilon_{\mathbf{k}} - i\delta} \times (\hat{V}(\mathbf{k}\mathbf{k}') \hat{V}(\mathbf{k}'\mathbf{k}) \hat{\rho}(\mathbf{k}) \\ &\quad - \hat{V}(\mathbf{k}\mathbf{k}') \hat{\rho}(\mathbf{k}') \hat{V}(\mathbf{k}'\mathbf{k})) - \frac{i/\hbar}{\varepsilon_{\mathbf{k}} - \varepsilon_{\mathbf{k}'} - i\delta} \\ &\quad \times (\hat{V}(\mathbf{k}\mathbf{k}') \hat{\rho}(\mathbf{k}') \hat{V}(\mathbf{k}'\mathbf{k}) - \hat{\rho}(\mathbf{k}) \hat{V}(\mathbf{k}\mathbf{k}') \hat{V}(\mathbf{k}'\mathbf{k})). \end{aligned} \quad (\text{B3})$$

Here, the real part of  $1/(\varepsilon_{\mathbf{k}'} - \varepsilon_{\mathbf{k}} - i\delta)$  corresponds to the small modification of electron states due to the impurity potential, which can be neglected. The imaginary part leads to actual transitions between states. They can be described with the equations

$$\begin{aligned} \frac{\partial \rho_{ij}(\mathbf{k})}{\partial t} &= \int \frac{V d\mathbf{k}'}{(2\pi)^3} \left( W_{ij,lm}^{(\text{in})}(\mathbf{k}, \mathbf{k}') \rho_{lm}(\mathbf{k}') - W_{ij,lm}^{(\text{out})}(\mathbf{k}, \mathbf{k}') \rho_{lm}(\mathbf{k}) \right), \end{aligned} \quad (\text{B4})$$

$$\begin{aligned} W_{ij,lm}^{(\text{in})}(\mathbf{k}, \mathbf{k}') \rho_{lm}(\mathbf{k}') &= \frac{2\pi}{\hbar} N_I \times V_{il}(\mathbf{k}, \mathbf{k}') \rho_{lm}(\mathbf{k}') V_{mj}(\mathbf{k}', \mathbf{k}) \delta(\varepsilon_{\mathbf{k}} - \varepsilon_{\mathbf{k}'}), \end{aligned} \quad (\text{B5})$$

$$\begin{aligned} W_{ij,lm}^{(\text{out})}(\mathbf{k}, \mathbf{k}') \rho_{lm}(\mathbf{k}) &= \frac{\pi}{\hbar} N_I \times [V_{in}(\mathbf{k}, \mathbf{k}') V_{nl}(\mathbf{k}', \mathbf{k}) \rho_{lm}(\mathbf{k}) \delta_{jm} \\ &\quad + \rho_{lm}(\mathbf{k}) V_{nm}(\mathbf{k}, \mathbf{k}') V_{nj}(\mathbf{k}', \mathbf{k}) \delta_{il}] \delta(\varepsilon_{\mathbf{k}} - \varepsilon_{\mathbf{k}'}). \end{aligned} \quad (\text{B6})$$

Here,  $N_I$  is the total number of impurities.  $W_{ij,lm}^{(\text{in})}(\mathbf{k}, \mathbf{k}')$  describes the electrons scattering from the state  $\mathbf{k}'$  to the state  $\mathbf{k}$ . Because both the initial and the final states of electrons are described with a  $2 \times 2$  density matrix,  $W_{ij,lm}^{(\text{in})}(\mathbf{k}, \mathbf{k}')$  is, therefore, a four-dimensional  $2 \times 2 \times 2 \times 2$  matrix.  $W_{ij,lm}^{(\text{out})}(\mathbf{k}, \mathbf{k}')$  is the out-scattering term that stands for the backward transition from  $\mathbf{k}$  to  $\mathbf{k}'$ . It is different from  $W_{ij,lm}^{(\text{in})}(\mathbf{k}, \mathbf{k}')$  because the spin is not conserved during the scattering. For a given density matrix  $\hat{\rho}(\mathbf{k}')$  of incident electrons,

$$W_{ij,lm}^{(\text{in})}(\mathbf{k}, \mathbf{k}') \rho_{lm}(\mathbf{k}') \quad (\text{B7})$$

represents the properties of the scattered ones. In particular, the results shown in Figs. 2(b) and 2(c) are calculated with Eq. (B7) where  $\hat{\rho}(\mathbf{k}') = (\hat{1} \pm \sigma_y)/2$  and  $\mathbf{k}' = (p_F/\sqrt{2}\hbar)(1, 0, 1)$ . The scattering probabilities correspond to  $\text{Tr} \hat{W}^{(\text{in})}(\mathbf{k}, \mathbf{k}') \hat{\rho}(\mathbf{k}') = W_{ii,lm}^{(\text{in})}(\mathbf{k}, \mathbf{k}') \rho_{lm}(\mathbf{k}')$ , and the spin polarization vector  $\mathbf{s}$  corresponds to  $\text{Tr} \sigma_r(\mathbf{k}) \hat{W}^{(\text{in})}(\mathbf{k}, \mathbf{k}') \hat{\rho}(\mathbf{k}') r^+(\mathbf{k}) = r_{ii}^+(\mathbf{k}) \sigma_{i_1 i_2} r_{i_2 j}(\mathbf{k}) W_{ji,lm}^{(\text{in})}(\mathbf{k}, \mathbf{k}') \rho_{lm}(\mathbf{k}')$ .

### APPENDIX C: BOUNDARY CONDITIONS FOR THE BOLTZMANN EQUATION

The approach (B4) is based on the wave functions  $\Psi_{\alpha}(\mathbf{k})$  defined in the main text. They correspond to the coherence of incident and specularly reflected electrons. However, in the bulk of the film this coherence is lost due to the scattering at the bulk impurities, and the Boltzmann equation approach is based on the distribution function  $\hat{f}(\mathbf{p})$  that neglects such a coherence.

To relate the two approaches, we consider the spin polarization generated per unit time. Because the kinetic equation is linear, we can decouple it into  $G_{\alpha}(\mathbf{p}) d\mathbf{p}$ —the spin polarization in the  $\alpha$  direction related to the reflected electrons with the momentum  $\mathbf{p}$ . In terms of the Boltzmann equation, it is expressed as follows:

$$G_{\alpha}(\mathbf{p}) d\mathbf{p} = \frac{d\mathbf{p}}{(2\pi\hbar)^3} \text{Tr} \hat{\sigma}_{\alpha} \hat{f}_2(\mathbf{p}) \frac{|p_z|}{m} S. \quad (\text{C1})$$

Here,  $\hat{f}_2(\mathbf{p})$  is taken at the interface and is assumed not to depend on the exact point of the interface.  $S$  is the interface area. Note that  $p_z$  is negative for the reflected electrons. In terms of Eq. (B4),  $G_{\alpha}(\mathbf{p}) d\mathbf{p}$  is equal to

$$\begin{aligned} G_{\alpha}(\mathbf{k}) d\mathbf{k} &= \frac{V d\mathbf{k}}{(2\pi)^3} \text{Tr} \hat{\tau}_{\mathbf{k}}^+ \hat{\sigma}_{\alpha} \hat{\tau}_{\mathbf{k}} \\ &\quad \times \int \frac{V d\mathbf{k}'}{(2\pi)^3} \left( W_{ij,lm}^{(\text{in})}(\mathbf{k}, \mathbf{k}') \rho_{lm}(\mathbf{k}') \right. \\ &\quad \left. - W_{ij,lm}^{(\text{out})}(\mathbf{k}, \mathbf{k}') \rho_{lm}(\mathbf{k}) \right). \end{aligned} \quad (\text{C2})$$

When  $\hat{f}_2 \ll \hat{f}_1 \ll \hat{f}_0$ , one can substitute  $\hat{\rho}(\mathbf{k})$  with  $\hat{f}_0(\hbar k_x, \hbar k_y, \hbar |k_z|) + \hat{f}_1(\hbar k_x, \hbar k_y, \hbar |k_z|)$  on the right-hand side of Eq. (C2). However,  $\hat{f}_0$  does not lead to spin polarization and can be dropped.

This allows us to derive the following boundary condition for  $\hat{f}_2$  at  $z = 0$ :

$$\begin{aligned} \hat{f}_2(\mathbf{p}) &= \frac{mV}{S|p_z|} \hat{r}(\mathbf{p}) \left[ \int \frac{V d\mathbf{p}'}{(2\pi\hbar)^3} \right. \\ &\quad \left. \times \hat{\mathcal{W}}\left(\frac{\mathbf{p}}{\hbar}, \frac{\mathbf{p}'}{\hbar}\right) (f_1(\mathbf{p}') - f_1(\mathbf{p})) \right] \hat{r}(\mathbf{p})^+. \end{aligned} \quad (\text{C3})$$

Here,

$$\mathcal{W}_{ij} = W_{ij,ll}^{(\text{in})} = W_{ij,ll}^{(\text{out})}, \quad (\text{C4})$$

and we took into account that  $\hat{f}_1 = f_1 \hat{1}$ .

- [1] R. Ramaswamy, J. M. Lee, K. Cai, and H. Yang, Recent advances in spin-orbit torques: Moving towards device applications, *Appl. Phys. Rev.* **5**, 031107 (2018).
- [2] A. Manchon, J. Železný, I. M. Miron, T. Jungwirth, J. Sinova, A. Thiaville, K. Garello, and P. Gambardella, Current-induced spin-orbit torques in ferromagnetic and antiferromagnetic systems, *Rev. Mod. Phys.* **91**, 035004 (2019).
- [3] Spin-orbit torque should not be confused with orbital torque that relies solely on the orbital degree of freedom; see, e.g., D. Lee, D. Go, H.-J. Park, W. Jeong, H.-W. Ko, D. Yun, D. Jo, S. Lee, G. Go, J. H. Oh, K.-J. Kim, B.-G. Park, B.-C. Min, H. C. Koo, H.-W. Lee, O. Lee, and K.-J. Lee, Orbital torque in magnetic bilayers, *Nat. Commun.* **12**, 6710 (2021); D. Go and H.-W. Lee, Orbital torque: Torque generation by orbital current injection, *Phys. Rev. Res.* **2**, 013177 (2020).
- [4] I. M. Miron, K. Garello, G. Gaudin, P.-J. Zermatten, M. V. Costache, S. Auffret, S. Bandiera, B. Rodmacq, A. Schuhl, and P. Gambardella, Perpendicular switching of a single ferromagnetic layer induced by in-plane current injection, *Nature (London)* **476**, 189 (2011).
- [5] L. Liu, O. J. Lee, T. J. Gudmundsen, D. C. Ralph, and R. A. Buhrman, Current-Induced Switching of Perpendicularly Magnetized Magnetic Layers Using Spin Torque from the Spin Hall Effect, *Phys. Rev. Lett.* **109**, 096602 (2012).
- [6] Y.-W. Oh, S.-h. Chris Baek, Y. M. Kim, H. Y. Lee, K.-D. Lee, C.-G. Yang, E.-S. Park, K.-S. Lee, K.-W. Kim, G. Go, J.-R. Jeong, B.-C. Min, H.-W. Lee, K.-J. Lee, and B.-G. Park, Field-free switching of perpendicular magnetization through spin-orbit torque in antiferromagnet/ferromagnet/oxide structures, *Nat. Nanotechnol.* **11**, 878 (2016).
- [7] I. M. Miron, T. Moore, H. Szabolcs, L. D. Buda-Prejbeanu, S. Auffret, B. Rodmacq, S. Pizzini, J. Vogel, M. Bonfim, A. Schuhl, and G. Gaudin, Fast current-induced domain-wall motion controlled by the Rashba effect, *Nat. Mater.* **10**, 419 (2011).
- [8] A. Hrabec, J. Sampaio, M. Belmeguenai, I. Gross, R. Weil, S. M. Chérif, A. Stashkevich, V. Jacques, A. Thiaville, and S. Rohart, Current-induced skyrmion generation and dynamics in symmetric bilayers, *Nat. Commun.* **8**, 15765 (2017).
- [9] A. V. Chumak, V. I. Vasyuchka, A. A. Serga, and B. Hillebrands, Magnon spintronics, *Nat. Phys.* **11**, 453 (2015).
- [10] M. Montazeri, P. Upadhyaya, M. C. Onbasli, G. Yu, K. L. Wong, M. Lang, Y. Fan, X. Li, P. Khalili Amiri, R. N. Schwartz, C. A. Ross, and K. L. Wang, Magneto-optical investigation of spin-orbit torques in metallic and insulating magnetic heterostructures, *Nat. Commun.* **6**, 8958 (2015).
- [11] M.-G. Kang, J.-G. Choi, J. Jeong, J. Y. Park, H.-J. Park, T. Kim, T. Lee, K.-J. Kim, K.-W. Kim, J. H. Oh, D. D. Viet, J.-R. Jeong, J. M. Yuk, J. Park, K.-J. Lee, and B.-G. Park, Electric-field control of field-free spin-orbit torque switching via laterally modulated Rashba effect in Pt/Co/ $\text{AlO}_x$  structures, *Nat. Commun.* **12**, 7111 (2021).
- [12] Y. Hibino, T. Moriyama, K. Hasegawa, T. Koyama, T. Ono, and D. Chiba, Spin-orbit precession effect in a Py/Pt/Co tri-layer structure detected by ferromagnetic resonance, *Appl. Phys. Express* **13**, 083001 (2020).
- [13] C. O. Avci, G. S. D. Beach, and P. Gambardella, Effects of transition metal spacers on spin-orbit torques, spin Hall magnetoresistance, and magnetic anisotropy of Pt/Co bilayers, *Phys. Rev. B* **100**, 235454 (2019).
- [14] S. Fukami, C. Zhang, S. DuttaGupta, A. Kurenkov, and H. Ohno, Magnetization switching by spin-orbit torque in an antiferromagnet-ferromagnet bilayer system, *Nat. Mater.* **15**, 535 (2016).
- [15] S. Shi, A. Wang, Y. Wang, R. Ramaswamy, L. Shen, J. Moon, D. Zhu, J. Yu, S. Oh, Y. Feng, and H. Yang, Efficient charge-spin conversion and magnetization switching through the Rashba effect at topological-insulator/Ag interfaces, *Phys. Rev. B* **97**, 041115(R) (2018).
- [16] M. DC, R. Grassi, J.-Y. Chen, M. Jamali, D. Reifsnnyder Hickey, D. Zhang, Z. Zhao, H. Li, P. Quarterman, Y. Lv, M. Li, A. Manchon, K. A. Mkhoyan, T. Low, and J.-P. Wang, Room-temperature high spin-orbit torque due to quantum confinement in sputtered  $\text{Bi}_x\text{Se}_{(1-x)}$  films, *Nat. Mater.* **17**, 800 (2018).
- [17] S. Alotibi, B. J. Hickey, G. Teobaldi, M. Ali, J. Barker, E. Poli, D. D. O'Regan, Q. Ramasse, G. Burnell, J. Patchett, C. Ciccarelli, M. Alyami, T. Moorsom, and O. Cespedes, Enhanced spin-orbit coupling in heavy metals via molecular coupling, *ACS Appl. Mater. Interfaces* **13**, 5228 (2021).
- [18] E. E. Krasovskii and E. V. Chulkov, Rashba polarization of bulk continuum states, *Phys. Rev. B* **83**, 155401 (2011).
- [19] I. V. Tokatly, E. E. Krasovskii, and G. Vignale, Current-induced spin polarization at the surface of metallic films: A theorem and an *ab initio* calculation, *Phys. Rev. B* **91**, 035403 (2015).
- [20] E. E. Krasovskii, Spin-orbit coupling at surfaces and 2D materials, *J. Phys.: Condens. Matter* **27**, 493001 (2015).
- [21] A. Droghetti and I. V. Tokatly, Current-induced spin polarization at metallic surfaces from first principles, *Phys. Rev. B* **107**, 174433 (2023).
- [22] A. Ganguly, K. Kondou, H. Sukegawa, S. Mitani, S. Kasai, Y. Niimi, Y. Otani, and A. Barman, Thickness dependence of spin torque ferromagnetic resonance in  $\text{Co}_{75}\text{Fe}_{25}/\text{Pt}$  bilayer films, *Appl. Phys. Lett.* **104**, 072405 (2014).
- [23] P. Li, L. J. Riddiford, C. Bi, J. J. Wissler, X.-Q. Sun, A. Vailionis, M. J. Veit, A. Altman, X. Li, M. DC, S. X. Wang, Y. Suzuki, and S. Emori, Charge-spin interconversion in epitaxial Pt probed by spin-orbit torques in a magnetic insulator, *Phys. Rev. Mater.* **5**, 064404 (2021).
- [24] H. Kronmüller and S. Parkin, *Handbook of Magnetism and Advanced Magnetic Materials*, 5 Volume Set (Wiley, New York, 2007).
- [25] M. Dyakonov, *Spin Physics in Semiconductors*, Springer Series in Solid-State Sciences (Springer, Berlin, 2008).
- [26] J. Sinova, S. O. Valenzuela, J. Wunderlich, C. H. Back, and T. Jungwirth, Spin Hall effects, *Rev. Mod. Phys.* **87**, 1213 (2015).
- [27] V. P. Amin and M. D. Stiles, Spin transport at interfaces with spin-orbit coupling: Formalism, *Phys. Rev. B* **94**, 104419 (2016).
- [28] V. P. Amin and M. D. Stiles, Spin transport at interfaces with spin-orbit coupling: Phenomenology, *Phys. Rev. B* **94**, 104420 (2016).
- [29] J. Borge and I. V. Tokatly, Boundary conditions for spin and charge diffusion in the presence of interfacial spin-orbit coupling, *Phys. Rev. B* **99**, 241401(R) (2019).
- [30] S.-h. C. Baek, V. P. Amin, Y.-W. Oh, G. Go, S.-J. Lee, G.-H. Lee, K.-J. Kim, M. D. Stiles, B.-G. Park, and K.-J. Lee, Spin currents and spin-orbit torques in ferromagnetic trilayers, *Nat. Mater.* **17**, 509 (2018).



- [31] V. P. Amin, J. Zemen, and M. D. Stiles, Interface-Generated Spin Currents, *Phys. Rev. Lett.* **121**, 136805 (2018).
- [32] A. Voskoboynikov, S. S. Liu, and C. P. Lee, Spin-dependent electronic tunneling at zero magnetic field, *Phys. Rev. B* **58**, 15397 (1998).
- [33] V. I. Perel', S. A. Tarasenko, I. N. Yassievich, S. D. Ganichev, V. V. Bel'kov, and W. Prettl, Spin-dependent tunneling through a symmetric semiconductor barrier, *Phys. Rev. B* **67**, 201304(R) (2003).
- [34] M. M. Glazov, P. S. Alekseev, M. A. Odnoblyudov, V. M. Chistyakov, S. A. Tarasenko, and I. N. Yassievich, Spin-dependent resonant tunneling in symmetrical double-barrier structures, *Phys. Rev. B* **71**, 155313 (2005).
- [35] K. Fuchs, The conductivity of thin metallic films according to the electron theory of metals, in *Mathematical Proceedings of the Cambridge Philosophical Society* (Cambridge University Press, Cambridge, 1938), Vol. 34, pp. 100–108.
- [36] L. A. Fal'Kovskii, Diffuse boundary condition for conduction electrons, *JETP Lett.* **11**, 138 (1970).
- [37] F. T. Vasko and O. E. Raichev, *Quantum Kinetic Theory and Applications: Electrons, Photons, Phonons* (Springer, New York, 2006).
- [38] R. F. Greene and R. W. O'Donnell, Scattering of conduction electrons by localized surface charges, *Phys. Rev.* **147**, 599 (1966).
- [39] E. M. Baskin and M. Entin, Electron scattering and the conductivity of a film with surface defects, *Sov. Phys. JETP* **30**, 252 (1970).
- [40] M. M. Glazov, Valley and spin accumulation in ballistic and hydrodynamic channels, *2D Mater.* **9**, 015027 (2022).
- [41] M. M. Glazov and L. E. Golub, Valley Hall effect caused by the phonon and photon drag, *Phys. Rev. B* **102**, 155302 (2020).
- [42] I. A. Ado, I. A. Dmitriev, P. M. Ostrovsky, and M. Titov, Anomalous Hall effect with massive Dirac fermions, *Europhys. Lett.* **111**, 37004 (2015).
- [43] L. Jin, K. Jia, D. Zhang, B. Liu, H. Meng, X. Tang, Z. Zhong, and H. Zhang, Effect of interfacial roughness spin scattering on the spin current transport in YIG/NiO/Pt heterostructures, *ACS Appl. Mater. Interfaces* **11**, 35458 (2019).